ISSN: 0067-2904
GIF: 0.851

Synthesis and Characterization of Gold Nanoparticles using 2-(2-methyl-5-amino -1*H*-imidazol-1-yl) ethanol

Ahlam Jameel Abdulghani*, May J. Kareem
University of Baghdad, College of Science, Department of Chemistry, Baghdad, Iraq

Abstract

Gold nanoparticles (Au NPs) have been synthesized via reduction of sodium tetrachloroaurate dihydrate ($NaAuCl_4.2H_2O$) with 2-(2-methyl-5-amino -1*H*-imidazol-1-yl) ethanol (2-MAE) in presence and absence of ascorbic acid as reducing and stabilizing agents. The resulting Au NPs were characterized by UV–Vis spectroscopy, scanning electron microscopy (SEM), atomic force microscopy (AFM), X-ray diffraction (XRD), FT-IR spectroscopy. The absorption spectra of gold nanoparticles solutions in the uv-visible and near IR regions were studied at different amine concentrations and pH media.

Keywords: Gold nanoparticles, Surface Plasmon resonance (SPR), SEM, AFM, UV–Vis spectrophotometry.

تحضير وتشخيص دقائق الذهب النانوية باستخدام (2-(2-مثيل -5-امينو-1-اميدازول)ايثانول

احلام جميل عبد الغني*، مي جودة كريم
جامعة بغداد، كلية العلوم، قسم الكيمياء، بغداد، العراق

الخلاصة

تم تحضير دقائق الذهب النانوية بطريقة كيميائية باختزال رباعي كلورواورات الذهب ($NaAuCl_4.2H_2O$) مع (2-(2-مثيل -5-امينو-1-اميدازول) ايثانول (2-MAE) بوجود وغياب حامض الاسكوربيك كعامل مختزل وعامل استقرارية . شخصت الدقائق النانوية الناتجة بواسطة مطيافية الاشعة فوق البنفسجية- المرئية وتحاليل المجهر الالكتروني الماسح ،ومجهر القوى الذرية ،وحيود الاشعة السينية و مطيافية FT-IR. .درست اطياف الامتصاص لمحاليل دقائق الذهب النانوية في المنطقة الفوق بنفسجية –المرئية و القريبة من تحت الحمراء للامين في تراكيز واوساط دالة حامضية مختلفة.

Introduction

The biological and therapeutic activity of nitroimidazoles has been suggested to depend upon the nitro group reduction process which leads to the formation of active intermediate species that interact with DNA of different microbes to produce biochemical damage [1]. Metronidazole (MZ) chemically 2-(2-methyl-5-nitro-1*H*-imidazol-1-yl) ethanol, is a member of the 5-nitroimidazole antimicrobials class and a broad spectrum antibiotic It has been used successfully in the treatment of antibiotic-associated pseudomembranous colitis, trichomoniasis and symptomatic amebiasis as well as the infections of *Helicobacter pylori* [2,3]. The spectrophotometric determination methods of MZ in the literature involves mainly the initial reduction of the nitro group to the amino group to form 2-(2-

*Email ahlamjameel@scbaghdad.edu.iq

methyl-5-amino -1*H*-imidazol-1-yl) ethanol (2-MAE) using different reducing agents [4-12]. Amines are used extensively as reductant and subsequent capping agents in the synthesis of metal nanoparticles, especially gold [13, 14]. Figure-1 shows the structures of (MZ) and (2-MAE).

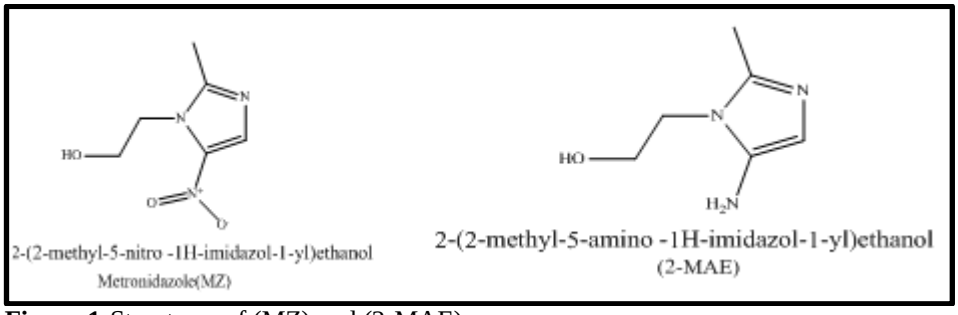

Figure 1-Structures of (MZ) and (2-MAE).

This work investigates the synthesis and characterization of 2-(2-methyl-5-amino -1*H*-imidazol-1-yl) ethanol (2-MAE) and the use of this compound in the synthesis of gold nanoparticles conjugates via the reduction of sodium tetrachloroaurate dihydrate ($NaAuCl_4.2H_2O$) in presence and absence of ascorbic acid as reducing and stabilizing agent.

Materials and Methods

Chemicals

All the following chemicals in this study were used as received from suppliers: Metronidazole (MZ) (99.98%) (SDI) Samarra Iraq, ascorbic acid ($C_6H_8O_6$) 99.7% (SCR, China), zinc powder (99%) (Fluka), sodium chloroaurate dihydrate ($NaAuCl_4.2H_2O$) Analar (99%) (BDH).

Instruments

The absorption spectra in the uv-visible region 200-1100 nm were recorded on a SHIMADZUE 1800 Double Beam UV-Vis spectrophotometer. Fourier Transform Infrared (FT-IR) spectra were recorded on Shimadzu FT-IR 8400S Fourier transforms, within the wavenumber region between 4000 and 200 cm^{-1} using KBr and CsI discs. Elemental microanalysis (C.H.N) was performed on Eurovector EA 3000A. ^{1}H-NMR spectra were performed by using: Bruker Ultra Shield 300 MHz NMR. Mass spectra measurements were performed using instrument: GC MS –QP 2010 VLTRA. Liquid Chromatography (LC) for the antibiotic MZ and reduced form (2-MAE) was performed on Shimadzu mode LC Column L7, UV319 nm, at chromatographic conditions: mobile phase containing methanol: water (20/80 v/v), flow rate 1mm/min. SEM images were acquired using KYKYEM-SEM model 3200. AFM images were obtained using AFM model CSPM (Scanning Probe Microscope). XRD measurements were performed using a Shimadzu XRD-6000 X-ray diffraction spectrometer.

Preparation of 2-(2-methyl-5-amino -1*H*-imidazol-1-yl) ethanol (2-MAE)

The reduction of metronidazole was performed following the procedure of Siddappa , et al [5] with modification. To a stirred solution of metronidazole (0.1g, $5.8x10^{-5}$ mole) in methanol (20 ml)was added hydrochloric acids(5N, 10 ml). Then zinc powder (0.5 g) was added to the acidic solution in portion with vigorous stirring. Hydrogen gas was evolved during addition and the color of solution turned immediately to yellow and then to colorless. The mixture was left under stirring for 1h until the bubbles of H_2 gas ceased. The solution was filtered to remove unreacted zinc powder which was washed several times with methanol. The total volume of the filtrate was made up to 100 ml with methanol so that the final concentration of the amine product (2-MAE) is ($5.84 x10^{-4}$M). The volume of the prepared solution was reduced to 30 ml by evaporation. The remaining solution was cooled and extracted with ethyl acetate. The acetate layer was separated and left overnight with anhydrous $MgSO_4$. Then cold ether was added to the faltered extracts. A brown oily precipitate was formed. The product was washed several times with ether followed by decantation. The remaining solvent was then evaporated by nitrogen gas to give a brown oily product. (yield 0.0432 g, 52.42 %). Boling point 165°C, CHN analysis, found [$C_6H_{11}N_3O$] $1.5H_2O$, : 42.432, 8.122, 24.855; calculated: 42.857, 8.333, 25.0; mass spectrum[m/z]:141 [$M^{+\cdot}$], 126[$M^{+\cdot}$ - CH_3], 124[$M^{+\cdot}$ –OH], 111[$M^{+\cdot}$ - CH_3 -NH], 96[$M^{+\cdot}$ – CH_2CH_2OH], 55 [$M^{+\cdot}$ – CH_2CH_2OH- C_2H_3N] ^{1}HNMR (δ,ppm): 7.090(C-H, imidazole ring), 6.9(NH_2), 4.136 (ethanolic chain OH,) 4.023(CH_2), 3.63 (CH_2), 2.51(CH_3);

Synthesis of GNPs

Preparation of Solutions for the synthesis of gold nanoparticles

A stock aqueous solution of the gold salt $NaAuCl_4.2H_2O$ (5.5×10^{-4} M) which contains (5.5×10^{-4} M) of Au^{3+} ions, was prepared by dissolving 0.1100 g of $NaAuCl_4.2H_2O$ in 50 ml distilled deionized water (DDW) in 50 ml volumetric flask. Ascorbic acid solution ($5.4\ x10^{-4}$ M) was freshly prepared by dissolving (0.0904 g) of ascorbic acid in 100 ml distilled deionized water (DDW) in 100 ml volumetric flask.

Effect of concentration of amine (2-MAE)

To study the effect of (2-MAE) concentration on GNPs synthesis, two series of solution were prepared. In the first series 0.5 ml aliquots of $NaAuCl_4$ aqueous solution ($5.5\ x10^{-4}$ M) were added to six 5ml volumetric flask containing different volumes of freshly prepared (2-MAE) ($3.06\ x10^{-4}$ M) (0.5, 1.0, 1.5, 2.0, 2.5 and 3.0 ml) . The volumes were then completed to 5 ml by distilled deionized water (DDW) with well mixing. The resulting molar concentrations of (2-MAE) are: 3.06, 6.12, 9.18, 12.24, 15.30, 18.36 x 10^{-5} M (samples 1-6 respectively)**,** while the concentration of Au(III) ions was kept constant at ($5.5\ x\ 10^{-5}$ M). The absorbance of each solution was measured to detect the position and intensity of SPR of Au NPs with time. In the second series 0.5 ml aliquots of freshly prepared aqueous solution of ascorbic acid ($5.4x10^{-4}$ M) were added to a set of eight volumetric flasks containing different volumes of freshly prepared (2-MAE) ($3.06\ x10^{-4}$ M) (0.5, 1.0, 1.5, 2.0, 2.5, 3.0, 3.5 and 4ml), followed by the addition of $NaAuCl_4$ ($5.5x10^{-4}$ M, 0.5 ml). The volumes were then completed to 5 ml by DDW with well mixing. The resulting molar concentrations of (2-MAE) were: : 3.06, 6.12, 9.18, 12.24, 15.30, 18.36 , 21.42, 24.48 x 10^{-5} M (samples (1-8)**,** while the concentration of added Au(III) ions and ascorbic acid were kept constant at (5.5 and $5.4\ x\ 10^{-5}$ M) , respectively. The absorbance of each solution was measured with time.

Effect of pH media

The synthesis of GNPs using the selected concentration of 2-MAE was studied spectrophotometrically at different pH values using HCl and NaOH for this purpose Two series of solutions were prepared. The first series consist of nine 5ml volumetric flasks containing 2-MAE ($3.06\ x10^{-4}$ M) to which were added 0.5 ml aliquots of $NaAuCl_4$ ($5.5x10^{-4}$ M) with pH adjusted to 2,3,4,5,6,7,8,9 and 10 values using HCl and NaOH for this purpose . The volumes were then completed to 5ml with vigorous mixing. The second series consists of ten 5ml volumetric flasks containing the same selected volume of 2-MAE ($3.06\ x10^{-4}$ M) and 0.5 ml aliquots of ascorbic acid solution ($5.4\ x10^{-4}$M). The same volumes of $NaAuCl_4$ ($5.5x10^{-4}$ M, 0.5 ml) were added with pH adjusted to 2,3,4,5,6,7,8,9,10 and 11. The volumes were completed to 5ml. The absorption spectra of all solutions were measured in the uv-visible region at different time intervals.

Results and Discussion:

Characterization of 2-MAE

Different methods have been reported in the literature on the reduction of MZ to 2-(2-methyl-5-amino -1*H*-imidazol-1-yl) ethanol (2-MAE) [4-12] referring to the difficulties in isolation characterization of the compound due to the susceptibility of the product to oxidation [9, 11]. In this work the results obtained from elemental CHN analysis, HNMR, and FTIR spectrophotometry were in good agreement with the chemical formula. The data obtained from ^{1}HNMR spectrum, and mass spectrum of 2-MAE came in agreement with the chemical structure [15- 17]. The FT-IR spectrum of (2-MAE) Figure-2 exhibited the disappearance of the bands assigned to the vibrational modes of asymmetrical and symmetrical stretching vibrations of NO_2 group which were located at 1537.16 and 1369.37 cm^{-1} respectively in the pure metronidazole [16,18], and the appearance of two bands observed at ν 3448.49, and 3336.27 cm^{-1}assigned to asymmetrical and symmetrical vibrations of primary amino group which confirms the reduction of NO_2 group to NH_2 group [9,19,20]. The bands appeared at around 3475.49 cm^{-1} was assigned to OH stretching modes of ethanolic group and hydrogen bonded water molecules associated with the amine molecule [16,18,21]. The bands assigned to the stretching modes of imidazole C-H and aliphatic CH_2 group were located at 2950.89 and 2840.95 cm^{-1} respectively [16,18]. The bands observed at 1633.59 and 1211.21 cm^{-1} were attributed to NH bending and C-N stretching vibrations of primary amine [17, 21, 22]. The band at around 1087.42cm^{-1} was attributed to C-O group stretching vibration of ethanolic group [18].

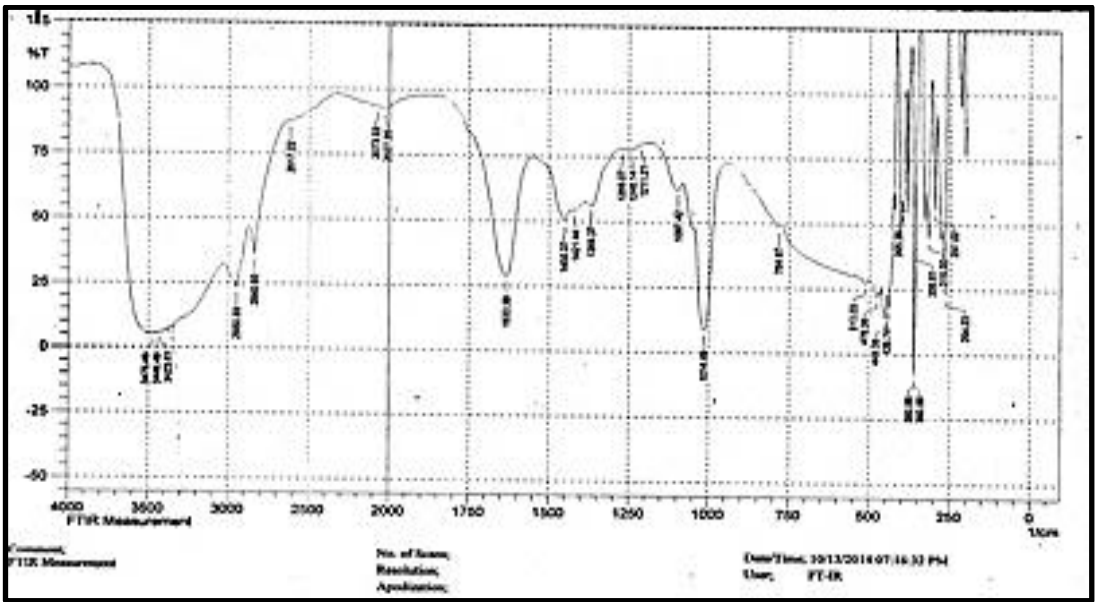

Figure 2- FTIR spectrum of 2-MAE

Figure-3 shows the LC chromatograph of the parent drug (MZ) and the reduced form (2-MAE). The peak of MZ, shown in Figure-3a appeared at retention time 7.789 min.. The chromatograph shown in Figure-3b exhibited almost the disappearance of this and the appearance of a high peak area at retention time 2.514 min. which supports the formation of the amino product.

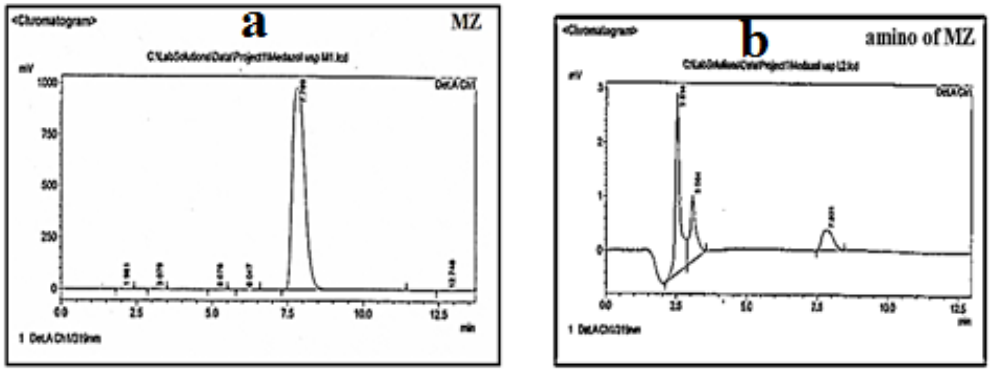

Figure 3- The LC chromatograms of a- MZ and b -(2-MAE) at conditions: mobile phase methanol: water 20:80(v/v), LC Column L7, detection wavelength 319 nm and flow rate 1mm/min.

Characterization of gold nanoparticles

Uv-Visible spectrophotometry

Figure-4 shows the spectra of (MZ) antibiotic, (2-MAE), $AuCl_4^-$ and gold nanoparticles prepared from mixing (2-MAE) and $AuCl_4^-$ aqueous solutions 3.6 and x 10^{-5} M and of ascorbic acid (AA) in aqueous solutions. The spectrum of MZ exhibited two high intensity bands at λ 221 and 310 nm attributed π-$\pi*$ transitions of imidazole ring [16, 17].

The spectrum of (2-MAE) displayed two high intensity bands at λ 220, and 240 nm (ε_{max} 43382, 26879 $L.mol^{-1}.cm^{-1}$ respectively) assigned to $\pi \rightarrow \pi^*$ transition of imidazole ring and a low intensity band at 393nm (ε_{max} 457, $L.mol^{-1}.cm^{-1}$) assigned to $n \rightarrow \pi^*$ transition of C=N group, [16,17,23]. The spectrum of ascorbic acid displayed a high intensity band at 253nm (ε_{max} 14509 $L.mol^{-1}.cm^{-1}$) which was attributed to $\pi \rightarrow \pi^*$ transition [24].

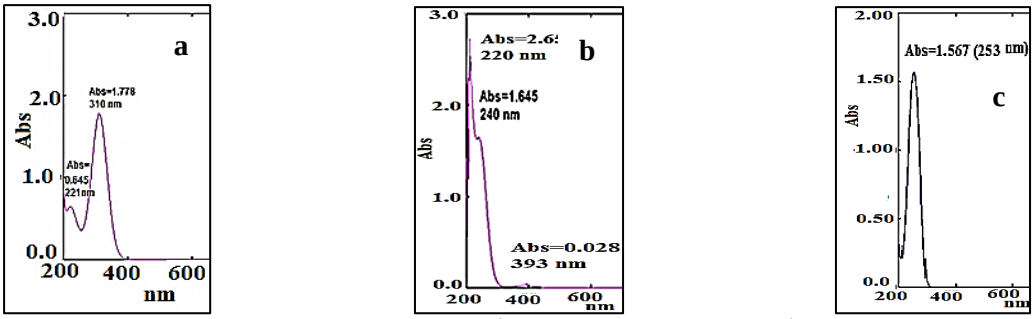

Figure 4- The absorption spectra of a- MZ (5.84 x10^{-4}M), b-(2-MAE) (3.06 x10^{-4} M and c- L- ascorbic acid (5.4 x10^{-4} M) in (DDW)

Optimization of reaction conditions

Concentration effect

Figure-5 show the absorption spectra of GNPs solutions prepared from aqueous solutions containing a constant concentration of Au(III) ions (5.5 x 10^{-5} M) and different concentrations of (2-MAE) (3.06, 6.12, 9.18, 12.24, 15.30, 18.36 x 10^{-5} M, samples 1-6 respectively). The spectrum of $AuCl_4^-$ solution (Figure (5a)) exhibited a high intensity band at λ 240 nm with a shoulder λ 290 nm assigned to LMCT transitions of tetrachloroaurate complex $AuCl_4^-$ [23]. On time of mixing, no color change was observed and the spectra showed no sign of SPB. After 24 h the solutions (1-4) exhibited purple violet colors, and their spectra displayed single peaks observed at λ 562, 564, 562, 570 nm respectively related to serface plasmon resonance (SPR) of spherical gold nanoparticles with the estimated size range 30-70 nm [25,26] .This indicates that gold nanoparticles have been synthesized and protected by (2-MAE). Figure (5a) shows the comparison between the spectra of (2-MAE), $AuCl_4^-$, and GNPs prepared from 3.06 x 10^{-5} M of (2-MAE) (solution 1). The slow rate of this reduction refers to slow growth of the seeding of GNPs [26] which may result from the formation of Au(II) and Au(I) ions. The intensity of SPBs were found to decrease with increasing concentration of 2-MAE. At high concentrations of 2-MAE (4,5,6) the solutions were yellowish in color and their spectra exhibited very low intensity peaks observed at λ 570, 582, 580 nm respectively which refers to formation of larger particle size of spherical gold NPs [26-29]. This was combined with gradual appearance of a new peak at 464 nm which may refer to the formation of a new product catalyzed by the oxidation of the synthesized GNPs and hence decreased the yield of GNPs. The optimum concentration for producing spherical GNPs by (2- MAE) was 3.06 x 10^{-5}M (solution 1) which was stable for more than one week

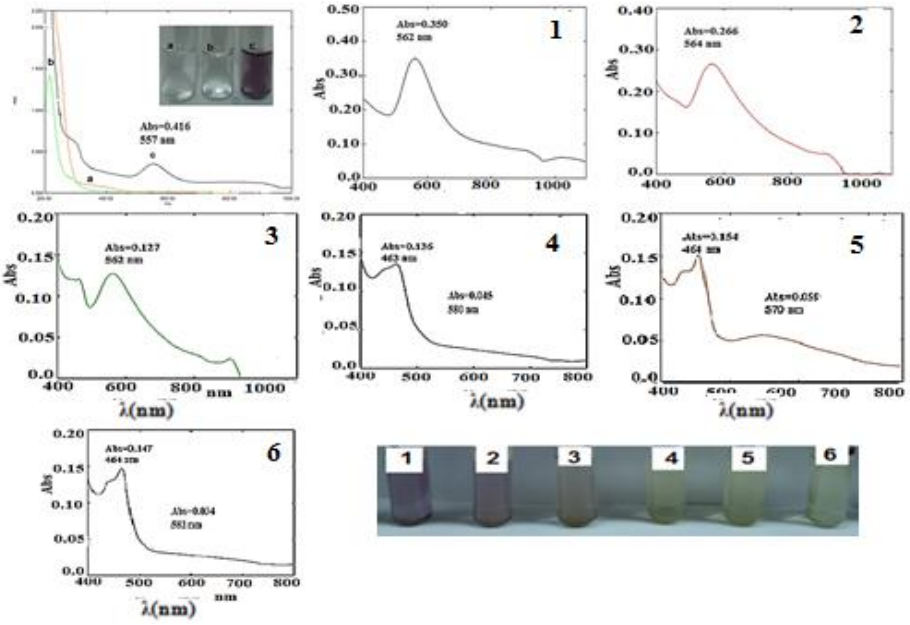

Figure 5- Absorption spectra and images of GNPs using 2-MAE (3.06, 6.12, 9.18, 12.24, 15.30, 18.36 x 10^{-5} M), $AuCl_4^-$ (5.5 x 10^{-5}M) (samples 1-6) after 24 h.

A size-controlled synthesis of gold nanoparticles may involve the oxidation of amine to give the monocations. Oxidation of the aromatic amine by Au (III) ions proceeds through the loss of electrons, which subsequently reduce the auric ions to gold atoms as was reported by Subramaniam, et al [13]. Accordingly for the reduction of Au (III) ions to GNPs by 2-MAE can be suggested as is illustrated by Scheme-1.

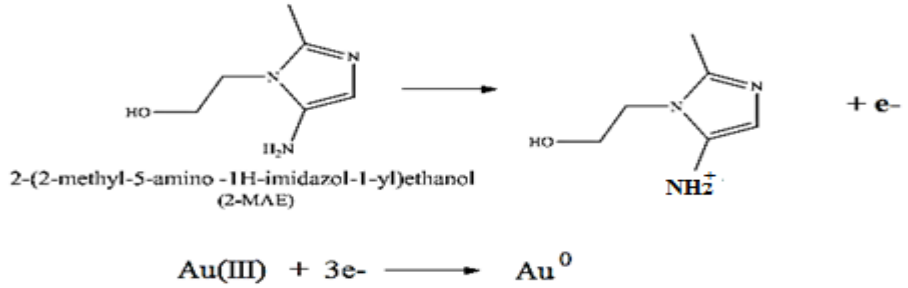

Scheme 1- The suggested mechanisms of the reduction of Au(III) ions by the amine (2-MAE).

In order to facilitate the reduction of Au(III) ion by the amine (2-MAE) the reduction should be catalyzed first by performing seeding to growth of AuNPs by a strong reducing agent which the resulting seeds allow for further reduction of Au(III)NPs on the surface of formed Au NPs [26] or by the addition of an antioxidants to stabilize and protect the synthesized GNPs against oxidation .

Synthesis of GNPs in presence of ascorbic acid

L- Ascorbic acid H_2A ($C_6H_8O_6$) has both one-electron and two-electron reducing properties and is reported to be irreversibly oxidized by metal ions via both inner- and outer-sphere redox mechanisms to DHA ($C_6H_6O_6$) [30]. As a result Au(III) ions will be reduced to either Au(I) or Au(0) by L-ascorbic acid (H_2A)($C_6H_8O_6$) [31].This indicates that the presence of ascorbic acid with (2-MAE) may speed up the reduction process. Figure-6 AA shows the uv-visible spectrum of gold nano- particles synthesized by ascorbic acid (5.4 $x10^{-4}$ M) which exhibited one single band observed at λ 573 nm corresponding to SPR of spherical gold nanoparticles [26-29]. The uv-visible spectra of GNPs prepared from solutions containing different concentrations of freshly prepared 2-MAE(3.06, 6.12, 9.18, 12.24, 15.30, 18.36 x 21.42, 24.48 x 10^{-5}M respectively) and constant concentrations of $AuCl_4^-$ (III) ions and AA (5.5 and 5.4 x 10^{-5} M respectively) Figure-6(1-8)(solutions 1-8) displayed two absorption bands. The first band was located in the visible region at λ 529, 531, 535, 541, 539, 542, 538, and 538nm respectively which correspond to the same position of SPR of spherical GNPs [26-28,] while the second peaks exhibited bathochromic shifts with increasing concentrations of (2-MAE) and appeared in the visible and near infra-red region (400-1100) at λ 620, 635, 640-1020, 748-998, 693-1017, 814-901, 819-1015, and 819- 910 nm respectively. The presence of two bands may refer to the formation of nonspherical GNPs aggregates or gold nano rods [32, 33]. The first three solutions (samples 1- 3) exhibited purple to violet colors after 1 h while the other five solutions showed violet color. Best performances were recorded by the first three solutions.

However, sample 1 was selected to represent the optimum concentration of (2-MAE) for synthesis of GNPs as the spectrum of this solution showed a higher energy of SPB in the visible region at λ 529 nm . The solution was stable for more than one week without a serious change in the position and intensity of SPB. These results show that presence of ascorbic acids with different concentration of amino play an important role in controlling both size and morphology of the synthesized GNPs.

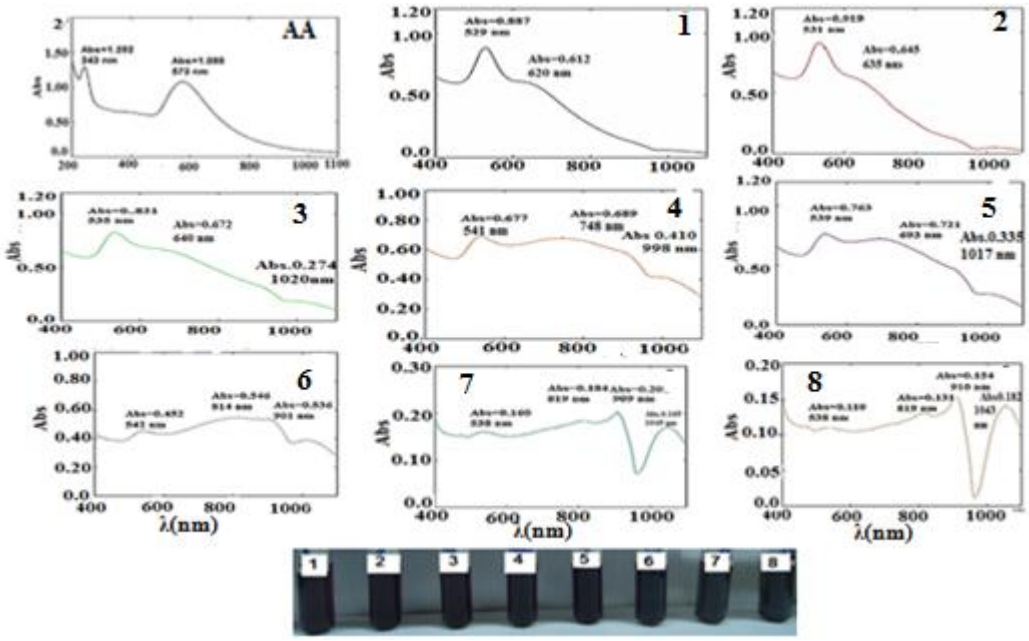

Figure 6- Absorption spectra and images of GNPs synthesized from ascorbic acid (AA) and 2-MAE (3.06, 6.12, 9.18, 12.24, 15.30, 18.36 , 21.42, 24.48 x 10^{-5}M, 1-8), $AuCl_4^-$ (5.5 x 10^{-5}M) with ascorbic acid (5.4 x 10^{-5}M) after 1 h.

Effect of pH media

Figures-7 shows the spectra of GNPs synthesized by (2-MAE) at the selected optimum concentration (3.06 x 10^{-5} M, sample 1) at different pH media (2-10) monitored by UV-visible spectrophotometry.

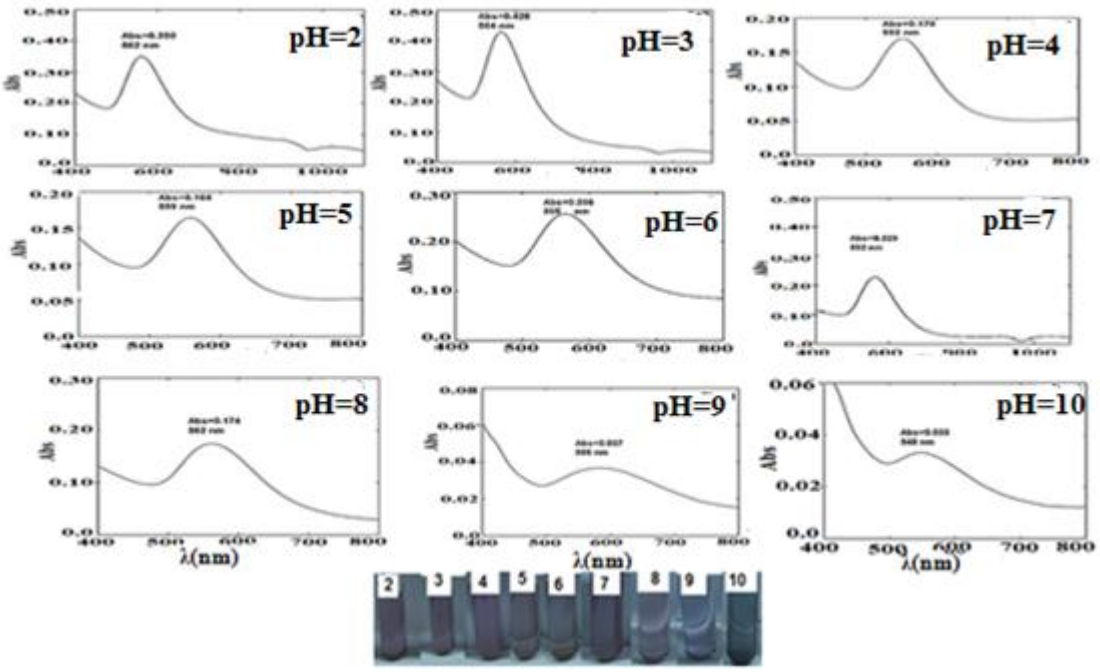

Figure 7- Absorption spectra and images of GNPs solutions prepared from $AuCl_4^-$ (5.5 x 10^{-5} M), (2-MAE) (3.06 x 10^{-5} M) at pH 2-7 after 24 h and pH 8, 9, 10 after 48 h.

At pH (2-7) the solutions showed a purple violet color after 24 h and the spectra of these solutions showed single absorption bands appeared at λ 562, 564, 552, 559, 565, and 562 nm respectively, with higher intensities of SPB at pH (2and 3), referring to the formation of large particle size of spherical gold nanoparticles [25,26], while the solutions at pH 8, 9, and 10 showed a purple violet color only after 48 h which indicates that increasing alkalinity of the solution decreased the rate of

reduction. The solutions at pH 4 was selected for stability study as the absorption band related to SPR in this solution appeared at shorter wavelength at λ 552 nm compared to that of pH (2, 3). The colloid was stable for more than 1 week, then intensity of SPB decreased and its position was shifted to longer wavelength. The synthesis of GNPs by ascorbic acid in presence of (2-MAE) at optimum concentration (3.06 x 10^{-5} M, sample 1) was studied spectrophotometrically at different pH media (2-11) and results are shown in Figure-8. The changes in colors for all solutions were observed after 1 h in contrast to those in absence of ascorbic acid which indicates that the presence of ascorbic acid increase the rate of reduction. The spectra of colloids showed two absorption bands in the visible region appeared at λ 531, 529, 528, 529, 528, 531, 528, 530 ,530, and 525nm respectively and second bands at λ 627, 655, 644, 646, 634, 630, 632, 631, 632, and 634nm respectively, referring to the formation of large sizes of non- spherical GNPs or gold nano rods [32,33].

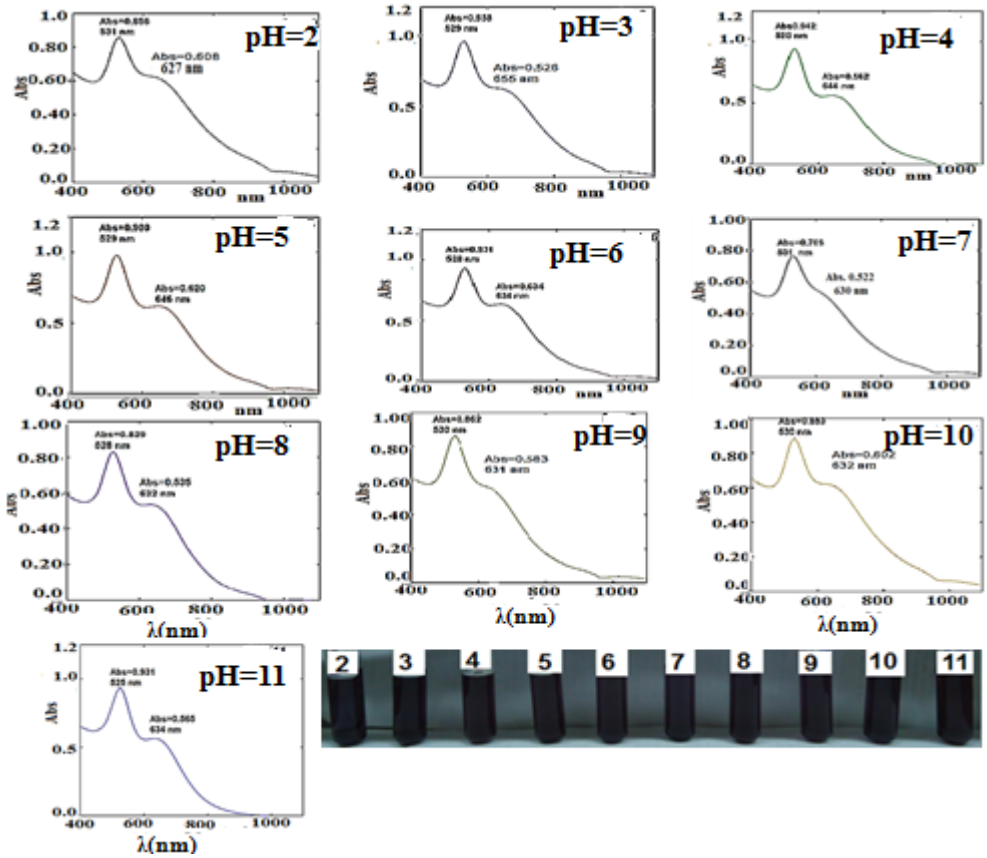

Figure 8- Absorption spectra and images of GNPs solutions prepared from (2-MAE) (3.06 x10^{-5} M), Au Cl_4^- (5.5x 10^{-5}M) and ascorbic acid (5.4 x 10^{-5} M) at pH 2 -11 after 1 h.

The optimum pH value for GNPs synthesis was at 11 which shows a high intensity absorption band of SPR at shorter wavelength λ 525 nm and λ 634 nm compared with the others. The increase in pH causes the formation of ascorbate anion which is more reducing than the corresponding acid.

Scanning electron microscopy (SEM) analysis.

Figure-9a shows the SEM micrograph and size distribution for amine (2-MAE) capped GNPs at concentrations of (2-MAE) (3.06 x 10^{-5} M) and $AuCl_4^-$ (5.5 x 10^{-5} M)) (sample 1) at pH=2 . The particles are characterized of having nearly uniform spherical and non-spherical shapes with a narrow size distribution of average particle size diameters around 25 nm**.** Figure-9b shows the SEM images and size distribution for (2-MAE) synthesized GNPs at the same concentrations but at pH 4. The particles had less uniform spherical shapes and wider size distribution with the average particle size diameters around 46 nm which reflects the effect of pH on the size and morphology of the synthesized GNPs.

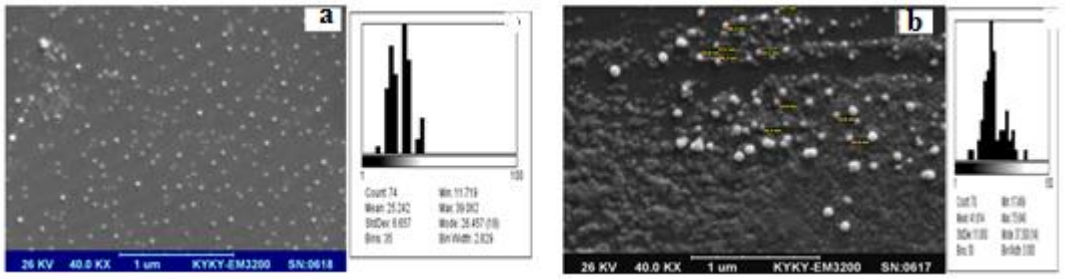

Figure 9- SEM images and particle size distributions GNPs prepared from (2-MAE) at a-pH 2 and b- pH 4(average size diameter 25 and46 nm respectively)

Figure-10a shows the SEM images and size distribution of GNPs prepared from (2-MAE) (3.06 x 10^{-5} M) and $AuCl_4^-$ (5.5x 10^{-5} M) in presence of ascorbic acid (5.4 x 10^{-5}M). At pH 2. The GNPs were of uniform spherical and nanocubes morphology with narrow size distribution of average size diameters around 26 nm**.** The SEM image at pH 4, Figure-10b showed highly regular shaped spherical GNPs with the average size diameters around 27.5 nm. This indicates that the addition of AA at this pH value improved the morphology by acting as antioxidant and capping agent.

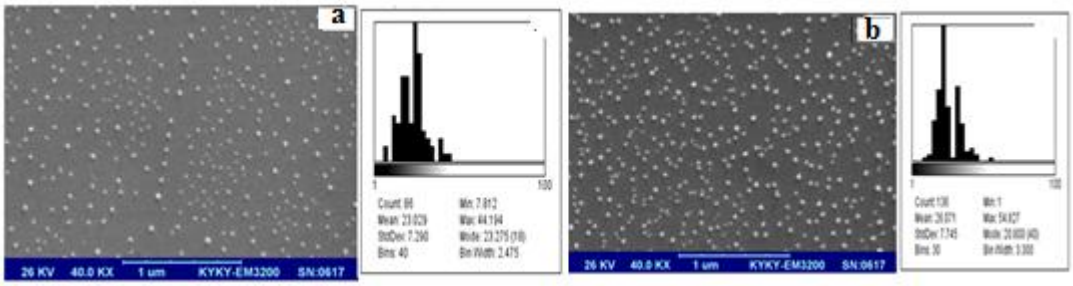

Figure 10- SEM images and particle size distribution GNPs prepared from amine (2-MAE) and ascorbic acid at a- pH 2 and b- pH 4 with (average size diameter 26 and 27.5 nm respectively)

Atomic force microscopy (AFM) analysis

Figures-11 and 12 show AFM images and granularity cumulation distribution chart of amine (2-MAE) capped gold nanoparticles(sample 1) (3.06 x 10^{-5} M), $AuCl_4^-$(5.5 x 10^{-5}M) at pH 2 and 4 respectively , the average particle diameters were around 79.81, 76.78nm respectively. The AFM pictures and granularity cumulation distribution charts of amine (2-MAE) capped gold nanoparticles (sample 1) using (2-MAE) (3.06 x10^{-5} M), $AuCl_4^-$ (5.5 x 10^{-5}M) in presence of ascorbic acid (5.4 x 10^{-5}M) Figures-13 and 14 at pH 2 and 4 respectively which gave average size diameter around 57.91 and 84.52 nm. The size difference between these results and those obtained from SEM micrographs may be attributed to the technical errors in the sample preparation techniques.

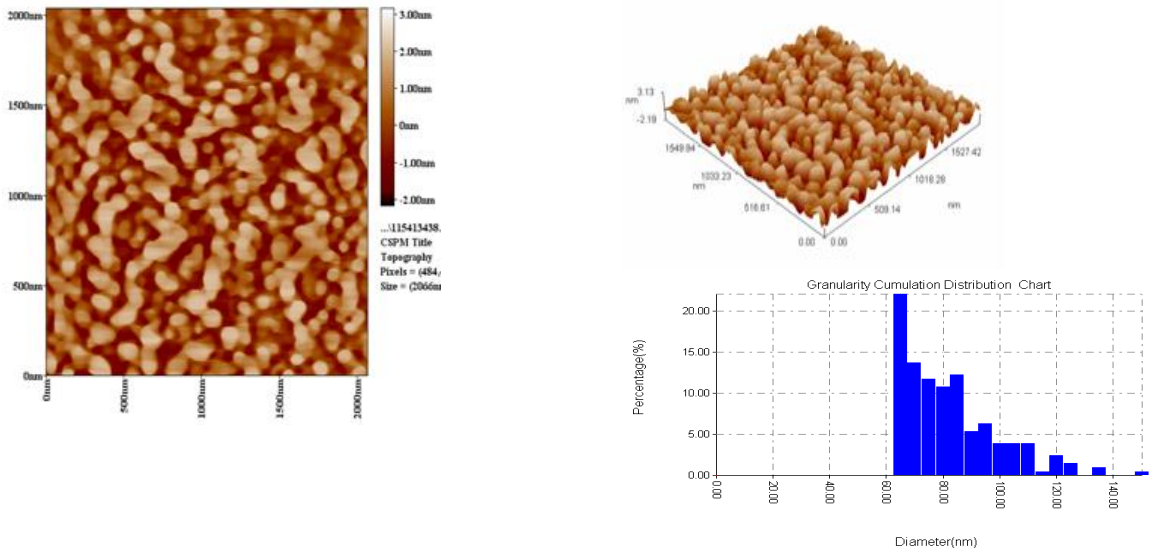

Figure 11- AFM 2D and 3D views and particle size distribution of (2-MAE) synthesized gold nanoparticles at pH 2 (average size diameter 79.81 nm).

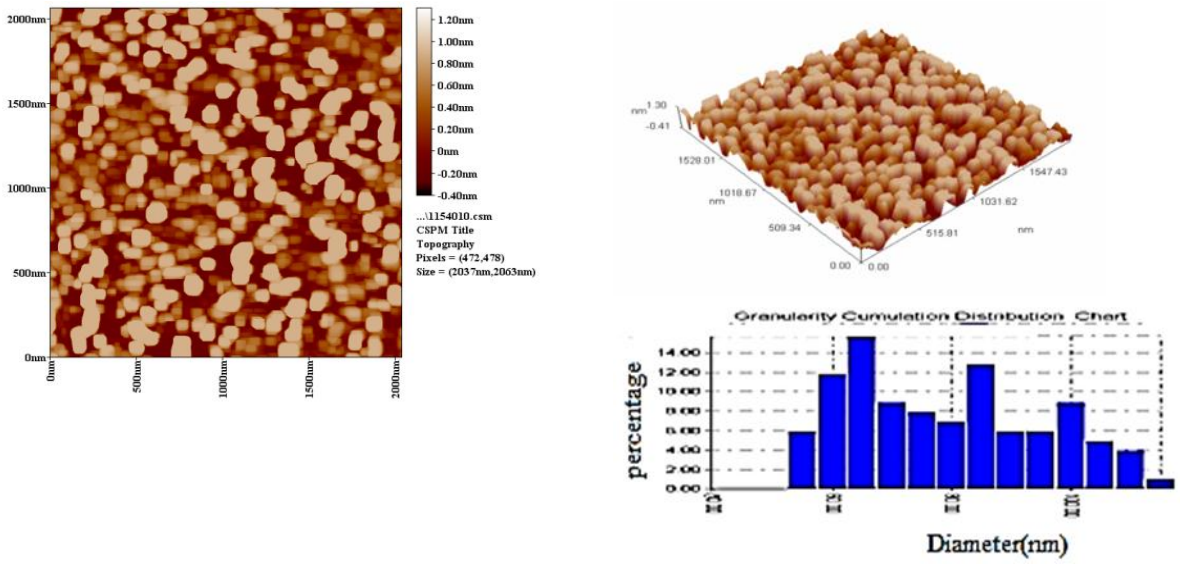

Figure 12- AFM 2D and 3D views and particle size distribution of gold nanoparticles prepared from amine (2-MAE) (3.06 x 10^{-5} M), $AuCl_4^-$(5.5 x 10^{-5} M), at pH 4 (average size diameter 76.78nm).

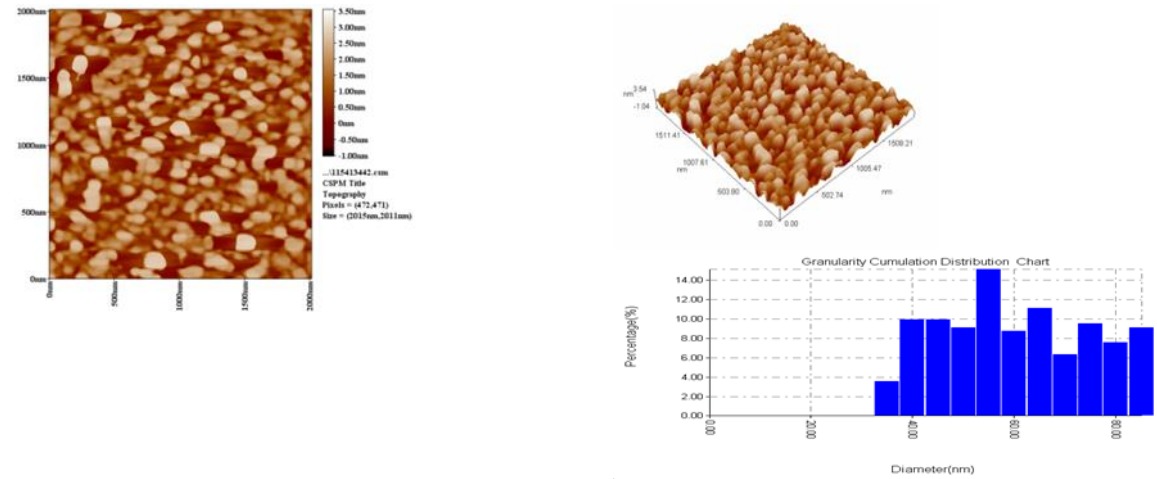

Figure 13- AFM 2D and 3D views and particle size distribution of gold nanoparticles prepared from (2-MAE) (3.06 x 10^{-5} M), $AuCl_4^-$(5.5 x 10^{-5} M), and AA (5.4 x 10^{-5}M) at pH 2 (average size diameter 57.91nm).

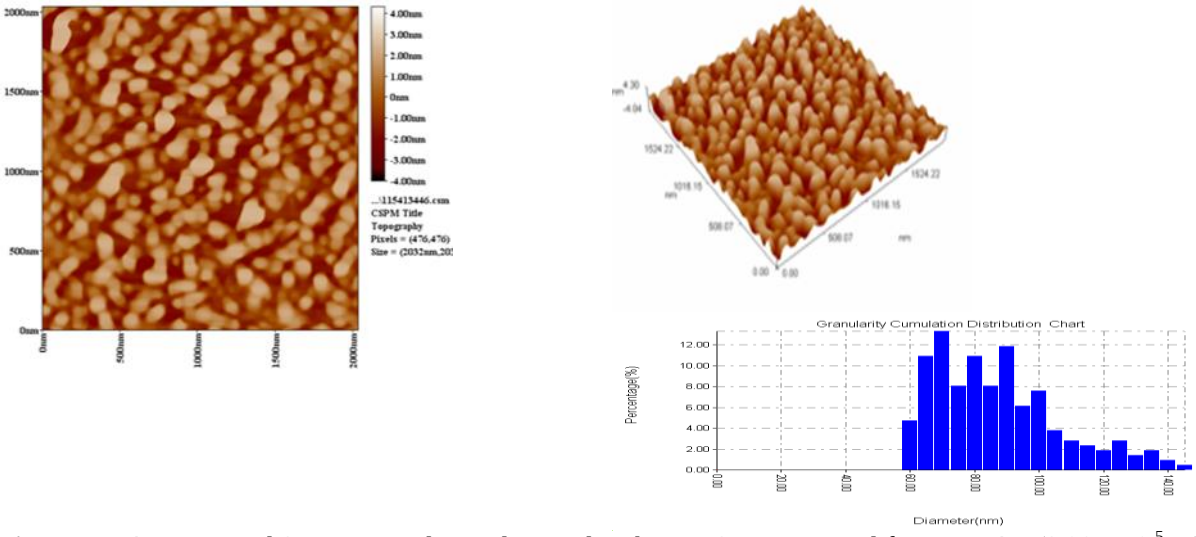

Figure 14- AFM 2D and 3D views and particle size distribution GNPs prepared from 2-MAE (3.06 x 10^{-5} M), $AuCl_4^-$(5.5x 10^{-5} M) and AA (5.4 x 10^{-5}M) at pH 4 (average size diameter 84.52 nm).

X-Ray diffraction (XRD) analysis

The XRD pattern of GNPs synthesized by (2-MAE) in presence of ascorbic acid is shown in Figure-15. Four diffraction peaks were observed at 2θ (38.76, 44.91, 65.14 and 77.51) degrees, corresponding to the planes (111), (200), (220) and (311) of face centered cubic (fcc) Au metal crystal lattice, respectively [26]. Average particle size has been estimated by using unmodified Debye-Scherrer formula equation [30, 34]

$$D = \frac{K \times \lambda}{\beta \cos \theta}$$

where 'D' is particle diameter size, θ is the Bragg angle, λ is the wavelength of the X ray used (0.154 nm), β is the breadth of the pure diffraction profile in radians on 2θ scale, K is a constant approximately equal to 0.90 and related both to the crystalline shape and to the way in which θ is defined. β is the Full Width at Half Maximum (FWHM) values. The value of D calculated from the (111) , (200), (220)and (311) reflections was 15.58nm, and the value of D calculated from the (111) reflection was 13.42 nm.

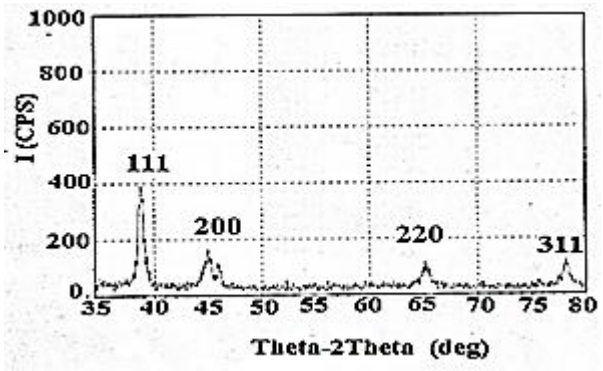

Figure 15- The XRD pattern of (2-MAE) capped Gold nanoparticles**.**

FT-IR spectrophotometry

The FTIR spectrum of (2-MAE) synthesized GNP_S shown in Figure-16a, exhibited a band at around 3558.42 cm^{-1} characteristic of the υ OH of lattice water [18]. The bands assigned to symmetrical and asymmetrical vibrations modes of amino group [9, 19, 20] were shifted to lower wavenumbers at 3427.27 $cm^{-1}$and 3311.55 cm^{-1}. The band assigned to OH stretching modes of ethanol group on imidazole ring were observed at wave number ranges at 3517- 3450 cm^{-1}. The band associated with N–H bending vibration of primary amines was located at 1649.02 cm^{-1} [18,21] while the band attributed to C-N stretching vibration of primary amine [21] and C-O of ethanol group were observed at 1257.50 cm^{-1} and 1058.85 cm^{-1} respectively. These results indicate that the amine ligand 2-MAE has been coordinated or covalently adsorbed on the surface of GNPs. The FTIR spectrum of GNP_S prepared in presence of (2-MAE) and ascorbic acid is shown in Figure-16b. The spectrum exhibited the disappearance of the peaks at 3525.63 and 3213.19 cm^{-1} assigned to OH stretching vibrations of L- ascorbic acid [18,35,36] and appearance of new bands at 1688.27, and 1674.10 cm^{-1} corresponding to C=O stretching vibrations [18,35,36] which refers to the oxidation of ascorbic acid as a result of GNPs synthesis. The band assigned to C=O stretching vibration observed at 1753.17 cm^{-1} in the spectrum of the free ligand [18,35,36] was shifted to 1735.81 cm^{-1}. The bands assigned to vibrational modes of amino group [9, 19, 20] of (2-MAE) were shifted to 3423.41 cm^{-1} and 3359.77 cm^{-1} respectively. The band assigned to OH stretching modes were located at wave number range 3565.42- 3550 and 3479.34 cm^{-1} respectively. The bands associated with N–H bending and C-N stretching vibrations of primary amine were shifted to higher wavenumbers and appeared at 1647.10 cm^{-1} [18,21] and 1263.29 cm^{-1} [21] respectively. The band at 1620 cm^{-1} may be assigned to the bending vibrations of ethanolic OH of imidazole ring. These results indicate that GNPs have been capped by ascorbic acid and the amine ligand.

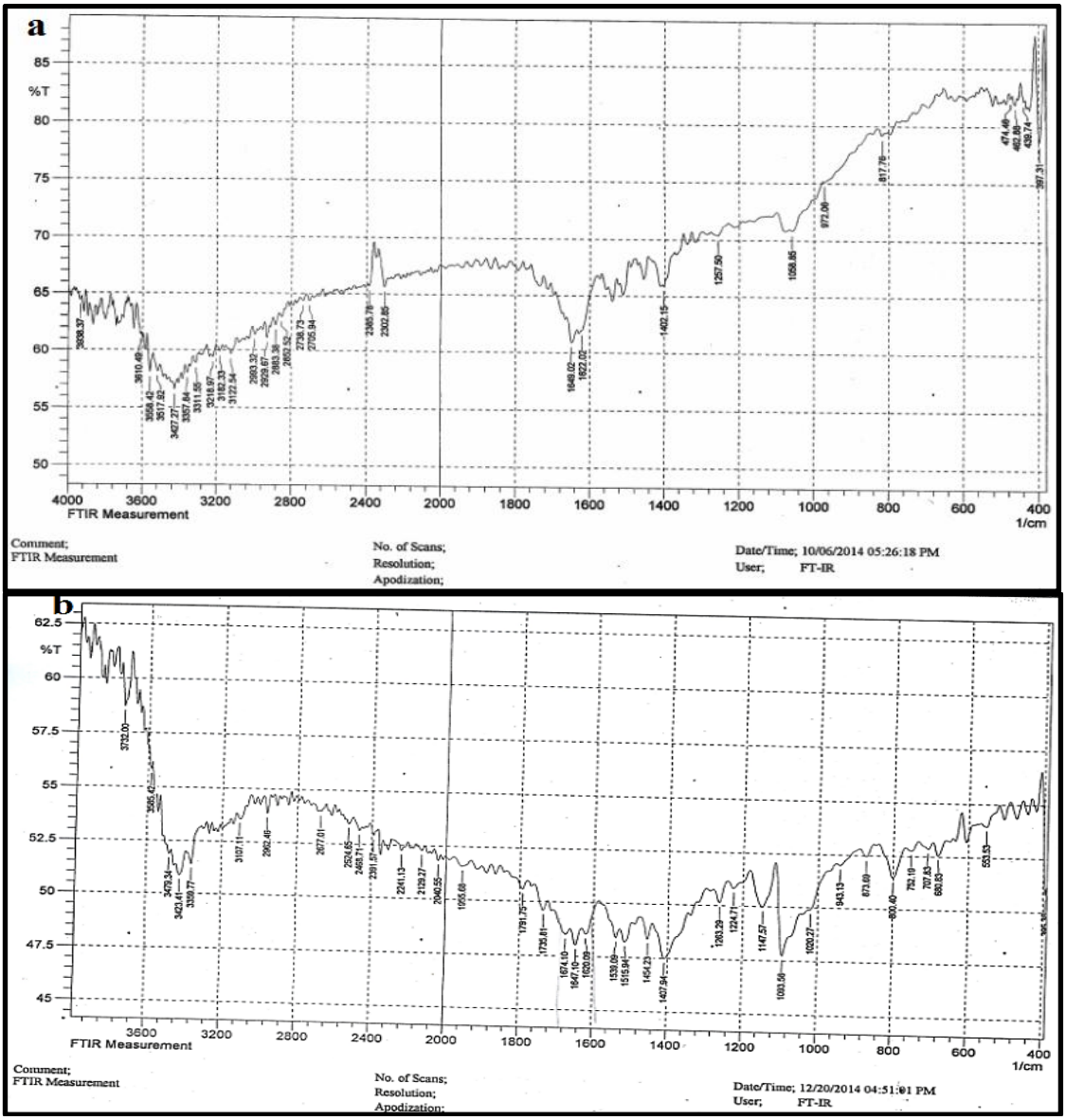

Figure 16- FTIR spectra of a- 2-MAE synthesized GNPs, and b- 2-MAE synthesized GNPs using ascorbic acid as reducing agent**.**

Biological Activity

The antibacterial activities of 2-MAE, GNPs- capped with (2-MAE) compared with the original metronidazole antibiotic at concentration (10^{-4} M) has been tested against four types of bacteria namely *Escherichia coli*, *Streptococcus pneumonia*, *Pseudomonas aeruginosa*, and *Staphylococcus aureus*, by using the agar diffusion method [37] .The inhibition zones created by (2-MAE) against the first three cultures (11, 20, 12 mm respectively) were comparable with those exhibited by MZ(11, 19, and13 mm respectively). The amine showed enhanced activity against *Staphylococcus aureus* (9 mm) to which MZ was inactive. On the other hand the 2-MAE/ GNPs exhibited very weak growth inhibition zones against all the studied bacteria (7.5, 8, 6,5 mm respectively) which indicates that conjugation of 2-MAE with GNPs decreased its antibacterial activity.

Conclusions

GNPs with different particle sizes have been synthesized by the reaction of (2-MAE) with $NaAuCl_4$ in aqueous solution at room temperature in the absence and presence of ascorbic acid as reducing and stabilizing agents at different concentrations of amino of MZ, and different pH media . Changes in concentrations and pH affect the size, morphology and stability of GNPs with time. The FTIR spectra of the prepared GNPs showed that the ligand molecules have been covalently attached on the surface of GNPs**.**

Acknowledgment

The authors wish to thank Dr. Abdul-Kareem M. Ali for performing the AFM analysis and Miss Muneera K. Ahmed and Mrs. Kareema Jaleal for performing the uv-visible spectral measurements.

References

1. Adegoke, O. A. **2011**. Spectrophotometric and thermodynamic studies of the charge transfer complexation of nitroimidazoles with chloranilic acid following metal hydride reduction. *Afr. J. Pure Appl .Chem* , 5(8), pp: 255-264.
2. Abdollahi, H., Savari, M., Zahedi, M. J., Moghadam, S. D., and Abasi, M. H. **2011**. A study of rdxa gene deletion in metronidazole resistant and sensitive helicobacter pylori isolates in Kerman, Iran, , *Jundishapur J. Microbiol*, 4(2), pp: 99-104.
3. Jorgensen, M. A., Manos, J., Mendz, G. L. and Hazell, S. L**. 1998**. The mode of action of metronidazole in *Helicobacter pylori:* futile cycling or reduction. *Journal of Antimicrobial* Chemotherapy, 41, pp: 67-75.
4. Saffaj,T., Charrouf, M., Abourriche, A ., Aboud,Y., Bennamara, A., Maoufoud, S. and Berrada, M. **2002**. Spectrophotometric determination of metronidazole in pharmaceutical preparations. *J Pharm Biomed Anal.* 15; 28 (3-4), pp :527-535.
5. Siddappa, K., Mallikarjun, M., Reddy, P. T. and Tambe, M. **2008**. Spectrophotometric determination of metronidazole through Schiff's base system using vanillin and PDAB reagents in pharmaceutical preparations. *Ecl. Quím, São Paulo,* 33(4), pp: 41-46.
6. Thulasamma, P and Venkateswarlu, P. **2009**. Spectrophotometric method for the determination of metronidazole in pharmaceutical pure and dosage forms. *Basayan J. Chem*, 2*(*4), pp: 865-868.
7. Adegoke, O. A. and Umoh, O. E. **2009**. A new approach to the spectrophotometric determination of metronidazole and tinidazole using p- dimethylaminobenzaldehyde . *Acta Pharm*, 59, pp: 407 – 419.
8. Fang, Z., Qiu, X., Chen, J. and Qin, X. **2010**. Degradation of metronidazole by nanoscale zero-valent metal prepared from steel pinkling waste liquor. *Applid Catalysis B:Environmental*, 100, pp:221-228.
9. Mustafa, Y. F., Al-Dabbagh, K . A. and Mohammed, M. F. **2008**. Synthesis of new metronidazole derivatives with suspected antimicrobial activity. *Iraq J. Pharm*, 7, 8((1), pp:34-41.
10. Ibrahim, W. H. and Bashir, W. A. **2012**. Spectrophotometric determination of metronidazole by prior reduction and subsequent diazotisation and coupling with N-(1-naphthyl) ethylenediamine–application to pharmaceutical preparations. *Raf. J. Sci.*, 23(3), pp: 78-93.
11. Dinesh, N. D., Nagaraja, P. and Rangappa, K. S. **2004**. Asensitive spectrophotometric assay for tinidazole and metronidazole using a Pd-C and formic acid reduction system. *Turk. J. Chem.*, 28, pp: 335-343.
12. Adegoke, O. A., Umoh,O. E. and Soyinka, J. O. **2010**. Spectrophotometric determination of metronidazole and tinidazole via charge transfer complexation using chloranilic acid. *J. Iran. Chem. Soc.*,7 (2), pp:359-370.
13. Subramaniam, C., Tom, R. T. and Pradeep, T. **2005**. On the formation of protected gold nanoparticles from AuCl4- by the reduction using aromatic amines. *Journal of Nanoparticle Research*, 7, pp: 209–217.
14. Yamamoto, M., Kashiwagi,Y. and Nakamoto, M . **2009**. Size-controlled synthesis of gold nanoparticles by thermolysis of a gold(I)-sulfide complex in the presence of . *Z. Naturforsch*., 64, pp: 1305 – 1311.
15. Ehlhardt, W. J., Beaulieu, B. B. and Goldman, P. **1987.** Formation of an amino reduction product of metronidazole in bacterial cultures lack of bactericidal activity. *Biochemical pharmacology* , 36(2), pp:259-264.
16. Chamundeeswari, S. P. V and Samuel, E. R. J. J. and Sundaraganesan ,N. **2011**. Theoretical and experimental studies on 2-(2-methyl-5-nitro-1-imidazolyl)ethanol. *European Journal of Chemistry*. 2 (2), pp: 136-145.
17. Obaleye, J. and Lawal, A. **2007**. Synthesis, characterization and antifungal studies of some metronidazole complexes**.** *J. Appl. Sci. Environ. Manage.*11(4), pp:15- 18**.**

18. Silverstein,R. M., Webster, E. X. and Kiley, D. J . **2005**. *Spectrometric Identification of Organic Compounds*. 7th ed, John Wiley and Sons Inc. ,Hodoken, USA, pp 1-502.

19. Ali Beg, A.A. and Qasir, A. J. **2014**. Synthesis and antimicrobial study of possible mutual prodrugs of amoxicillin and metronidazole by direct and indirect coupling through spacer. *Iraqi J Pharm Sci* , 23(1), pp:1-6.

20. Kapoor, V. K., Dubey, S. and Mahindroo, N. **2000**. Preparation, antibacterial evaluation and mutagenicity of some metronidazole derivatives. *Indian Journal of Chemistry*, 39, pp: 27-30 .

21. Coates, J. . **2000**. Interpretation of infrared spectra, a practical approach , In *Encyclopedia of Analytical Chemistry*, R.A. Meyers (Ed.), John Wiley & Sons Ltd, Chichester , pp: 10815–10837.

22. Huang, C. Chiu, P, Wang, Y. Meen,T . and Yang, C. **2007**. Synthesis and characterization of gold nanodog bones by the seeded mediated growth method. *Nanotechnology*, 18, pp: 1- 6.

23. Abdulghani, A. J., Jasim, H. H. and Al-kadumi, A. S. H. **2012**. Molecular and atomic spectrophotometry and high performance liquid chromatographic determination of metronidazole in dosage forms via complex formation with Au(III) and Hg(II) ions in solutions. *J. Chem. Pharm. Res*., 4(7), pp: 3749-3758.

24. Lawal, A., Obaleye, J.A., Oyeleke, S. A. and Amolegbe, S.A. **2009**. Synthesis and antibacterial studies of mixed metronidazole- vitamin c metal complexes. *Centrepoint* (Science Edition), 15 ,pp: 54 -59.

25. Ghosh, D., Sarkar, D., Girigoswami, A. and Chattopadhyay, N. **2010**. Fully standardized method of synthesis of gold nanoparticles of desired dimension in the range 15 nm–60 nm. *Journal of Nanoscience and Nanotechnology*, 10 , pp:1–6.

26. Niu, J., Zhu,T. and Liu, Z. **2007**. One-step seed-mediated growth of 30–150 nm quasispherical gold nanoparticles with 2-mercaptosuccinic acid as a new reducing agent. *Nanotechnology* , 18(325607) , pp :1-7.

27. Wang, B., Chen, K. , Jiang, S., Reincke, F., Tong, W., Wang, D. and Gao,C**. 2006**. Chitosan-mediated synthesis of gold nanoparticles on patterned poly (dimethyl siloxane) surfaces. *Biomacromolecules*, 7, pp: 1203-1209.

28. Li, C., Li, D., Wan,G. Xu, J. and Hou,W. **2011**. Facile synthesis of concentrated gold nanoparticles with low size-distribution in water: temperature and pH controls. *Nanoscale Research Letters*, 6 (440), pp: 1-10.

29. Johan,M. R., Chong, L. C. and Hamizi, N. A. **2012**. Preparation and stabilization of monodisperse colloidal gold by reduction with monosodium glutamate and poly (Methyl Methacrylate. *Int. J. Electrochem. Sci*.,7, pp: 4567 – 4573.

30. Elizondo, N., Segovia, P. , Coello, V., Arriaga, J., Belmares, S. , Alcorta, A. , Hernández, F., Obregón, R., Torres, E.and Paraguay, F. **2012**. Green synthesis and characterizations of silver and gold nanoparticles. *Green Chemistry Environmentally Benign Approaches*, 51(9), pp: 140-156.

31. Zumreoglu-Karan, B. **2009.** A rationale on the role of intermediate Au(III)–vitamin C complexation in the production of gold nanoparticles, , *J Nanopart , Res.* , 11 ,pp: 1099–1105.

32. Sama, A. K., Sreeprasad, T. S. and Pradeep, T. **2010**. Investigation of the role of $NaBH_4$ in the chemical synthesis of gold nanorods. *J. Nanopart. Res*., 12, pp:1777–1786.

33. Khalavka,Y., Becker, J., and Sonnichsen, C. **2009**. Synthesis of rod-shaped gold nanorattles with improved plasmon sensitivity and catalytic activity. *J. Am. Chem. Soc.*, 131(9), pp: 1871–1875.

34. Prema, P. and Thangapanaiyan, S. **2013**. In- vitro antibacterial activity of gold nanoparticles capped with polysaccharide stabilizing agents. *Int. J. Pharm. Pharm. Sci*., 5(1) , pp: 310-314.

35. Singha,P., Singha , N. P. and Yadavb, R. A. **2010**. Study of the optimized molecular structures and vibrational characteristics of neutral L-Ascorbic acid and its anion and cation using density functional theory. *J. Chem. Pharm. Res.*, 2(5), pp: 656-681.

36. Dabbgh, H. A., Azami, F., Farrokhpour, H., Chermahini, A. N. **2014**. Uv-Vis., NMR and FT-IR spectra of tautomers of vitamin C. Experimental and DFT Calculations. *J. Chil. Chem. Soc*., 59(3), pp:2588-2594.

37. Baccigalupi, L. Donato, A. Parlato, M. Luongo, D. Carbone, V. and Rossi, M. **2005**. Two small, surface-associated factors mediate adhesion of a food-isolated strain of *Lactobacillus fermentum* to cacocell. *Research Microbial*, 156, pp: 830-836.